

Andrzej Urbaś  
Marek Szczotka

## THE INFLUENCE OF THE FRICTION PHENOMENON ON A FOREST CRANE OPERATOR'S LEVEL OF DISCOMFORT

### WPŁYW ZJAWISKA TARCIA NA POZIOM DYSKOMFORTU PRACY OPERATORA ŻURAWIA LEŚNEGO\*

*A mathematical model of a forest crane that is suitable for dynamics analysis of its operation cycle is presented in this paper. The flexibility of the operator's seat, drives and supports is taken into account. Joint coordinates are applied to describe the motion of the links together with the homogeneous transformations technique. Lagrange equations of the second order are used when deriving the equations of motions. Joint forces and torques are determined based on recursive Newton-Euler algorithms. These joint forces are then used in the LuGre friction model, which allows to calculate the friction coefficients and friction forces. Numerical analyses performed here show the influence of various friction forces on the vibration level as perceived by the operator of the crane. The level of discomfort is discussed based on standards commonly used in the vehicle and transportation industry for evaluations of vibration comfort.*

**Keywords:** crane dynamics, friction, seat vibrations.

*W niniejszym artykule przedstawiono model matematyczny żurawia leśnego, który jest stosowany do analizy dynamiki cyklu jego pracy. Uwzględniono podatność podparcia fotela operatora, napędów oraz podpór. Do opisu ruchu członów stosuje się współrzędne złączowe i macierze przekształceń jednorodnych. Do wyprowadzenia równań ruchu modelu żurawia zastosowano podejście bazujące na formalizmie równań Lagrange'a drugiego rodzaju. Siły i momenty węzłowe są określone na podstawie rekurencyjnego algorytmu Newtona-Eulera. Siły te są następnie wykorzystywane w modelu tarcia LuGre, który pozwala obliczyć współczynniki i siły tarcia. Przeprowadzone analizy numeryczne pokazują wpływ różnych sił tarcia na poziom drgań odczuwany przez operatora żurawia. Poziom dyskomfort operatora wywołany przez drgania maszyny został oszacowany w oparciu o często stosowane w przemyśle samochodowym i transportowym odpowiednie standardy.*

**Słowa kluczowe:** dynamika żurawia, tarcie, drgania siedzenia.

#### Nomenclature

$b, c, s, d, j$	– flexible supported base, crane, seat, drive and joint indexes, respectively
$(c, l) \Big _{l=1, \dots, 7}$	– link index
$g$	– acceleration of gravity
$l^{(c, l)}$	– length of link
$m^{(b)}, m^{(c, l)}, m^{(s)}$	– masses of bodies
$n_b$	– number of bodies
$n_{dof}$	– number of generalised coordinates describing the motion of system
$\tilde{n}_{dof}^{(c, l)}$	– number of generalised coordinates describing the motion of link $(c, l)$ with respect to link $(c, l-1)$
$n_{dof}^{(b)}, n_{dof}^{(c, l)}, n_{dof}^{(s)}$	– number of generalised coordinates describing the motion of link with respect to reference system $n_{dof}^{(c, l)} = n_{dof}^{(b)} + n_{dof}^{(c, l-1)} + \tilde{n}_{dof}^{(c, l)}, n_{dof}^{(c, l)} = 0$
$s_{\beta}^{(sup_{\alpha, i})}, d_{\beta}^{(sup_{\alpha, i})} \Big _{\substack{\alpha \in \{b, s\} \\ \beta \in \{x, y, z\}}}$	– stiffness and damping coefficients of support

(\*) Tekst artykułu w polskiej wersji językowej dostępny w elektronicznym wydaniu kwartalnika na stronie [www.ein.org.pl](http://www.ein.org.pl)

$s^{(d,i)}, d^{(d,i)}$	–	stiffness and damping coefficients of drive
$t_f^{(j,i)}, f_f^{(j,i)}$	–	friction torque in revolute joint, friction force in prismatic joint, respectively
$sup_{\alpha \in \{b,s\}}$	–	support index
$t^{(d,i)}, f^{(d,i)}$	–	driving torques and force, respectively
$\mathbf{r}_A^{(a)} = \begin{bmatrix} x_A^{(a)} & y_A^{(a)} & z_A^{(a)} & 1 \end{bmatrix}^T$	–	vector of position of point $A$ defined in the local coordinate system of link $a$
$\mathbf{H}^{(b)}, \mathbf{H}^{(c,l)}, \mathbf{H}^{(s)}$	–	pseudo-inertia matrices
$\tilde{\mathbf{T}}^{(c,l)}$	–	homogeneous transformation matrix from the local coordinate system of link $(c,l)$ to the system of link $(c,l-1)$
$\mathbf{T}^{(b)}, \mathbf{T}^{(c,l)}, \mathbf{T}^{(s)}$	–	homogeneous transformation matrices from the local coordinate systems to reference system $\mathbf{T}^{(c,l)} = \mathbf{T}^{(b)}\mathbf{T}^{(c,l-1)}\tilde{\mathbf{T}}^{(c,l)}, \mathbf{T}^{(c,0)} = \mathbf{I}$ $\mathbf{T}_i = \frac{\partial \mathbf{T}}{\partial q_i}, \mathbf{T}_{i,j} = \frac{\partial^2 \mathbf{T}}{\partial q_i \partial q_j}$

**Friction parameters**

$\sigma_0^{(j)} = (\sigma_{0,i}^{(j)})_{i=1,\dots,7}, \sigma_1^{(j)} = (\sigma_{1,i}^{(j)})_{i=1,\dots,7}$	–	vectors of stiffness, damping and viscous friction coefficients of bristles, respectively
$\sigma_2^{(j)} = (\sigma_{2,i}^{(j)})_{i=1,\dots,7}$		
$\mathbf{z}^{(j)} = (z_i^{(j)})_{i=1,\dots,7}$	–	vector of deflections of bristles
$\boldsymbol{\mu}^{(j)} = (\mu_i^{(j)})_{i=1,\dots,7}$	–	vector of friction coefficients
$\boldsymbol{\mu}_s^{(j)} = (\mu_{s,i}^{(j)})_{i=1,\dots,7}, \boldsymbol{\mu}_k^{(j)} = (\mu_{k,i}^{(j)})_{i=1,\dots,7}$	–	vectors of static and kinetic friction coefficients, respectively
$\dot{\mathbf{q}}_S^{(c)} = (\dot{q}_{S,i}^{(c)})_{i=1,\dots,7}$	–	vector of transition velocities between friction regimes

**Parameters used for comfort assessment (BS 6841, 1987, ISO 2631-1, 1997)**

$y(t)$  Time history of a signal (discrete, calculated by the numerical simulation). The signal  $y(t)$  should be filtered using the frequency filters.

$RMS = \sqrt{\frac{1}{T} \int_0^T y^2(t) dt}$  Root-Mean-Square describes the energetic content of a vibrational signal,  $T$  is the time period of vibration.

$C_f = \frac{\max(|y(t)|)}{RMS}$  Crest factor, to be used in presence of shocks (short high magnitude transient events).

$RMQ = \sqrt[4]{\frac{1}{T} \int_0^T y^4(t) dt}$  Quad-Mean-Square, similar measure to  $RMS$ , but better describes the effect of vibration discomfort when  $C_f > 9$ .

$K = \frac{1}{n\sigma^4} \sum_{i=1}^n (y_i - \bar{y})^4$  Kurtosis, used for highly impulsive time domain signals, where  $n$  is the number of discrete data,  $\sigma$  is the standard deviation,  $\bar{y}$  is the average value of the analyzed signal.

$V DV = 4 \sqrt[4]{\int_0^T y^4(t) dt}$  Vibration dose value, gives a measurement of a cumulative vibration level received over a time period (often 8hr or 16hr). Location and direction dependent filters to be applied.

$T_{15} = \left(\frac{15}{VDV}\right)^4 t$  The duration in seconds, required to reach the value of  $VDV = 15ms^{-1.75}$  which is defined as a severe discomfort. Parameter  $t$  is the duration of measured or calculated signal.

**1. Introduction**

Crane control problems are becoming increasingly important for designers and operators. The efficiency of load handling and increased safety and level of comfort for all personnel involved and crane operators are the main driving factors for developments in this field. For this purpose, modern machines are equipped with quite advanced and expensive sensors and other control devices. Computer simulations, even in the very early design phase, are a very useful approach that aims to reduce the overall cost and to eliminate some errors that can be predicted without building real physical prototypes of the crane. Moreover, one can easily simulate complex machine behaviour without the risk of damage or injuries. In this context, many crane models have been developed with varying complexity and level of details.

In this work, a mathematical model of a grab crane is presented [12, 13, 18, 22-24, 19, 20, 26-30]. Its main purpose is to investigate dynamics during various operation modes and handling scenarios, including estimation of loads, load motion, drive system control and others. The flexibility of the support system [22-24, 26-30], which is modelled as one-dimensional spring-damping elements, is taken into account in the mathematical model. In the similar way a flexible system is built to represent the operator's seat connection to the crane column. In the crane model developed here, all drive units also have flexible features [26-30]. Homogeneous transformation and joint coordinates are applied to describe the geometry of the crane units [7, 14, 15]. Equations of motion can be derived based on methods and algorithms presented in [11, 32]. The Runge-Kutta method of the fourth order is applied for integration of the governing equations of motion, with constant time step. In order to determine the joint forces and torques, which are necessary to calculate the friction forces and torques, each integration time step involves recursive loops defined as the Newton-Euler recursive dynamics task [5]. The friction coefficients for each kinematic pair are calculated by applying the LuGre friction model [1, 2, 17, 21] which takes into account pre-sliding displacement [4], as well as the Stribeck effect [25], among other features.

The influence of friction on forest crane dynamics has been discussed in some previous papers. The Dahl friction model was investigated in [27], while works [29, 30] concentrated on the LuGre friction model.

The analyses performed here concentrated on the dynamic properties of the crane with particular interest in the operator's seat properties during selected modes of operation. The LuGre friction model, with two different friction levels characterised by joint conditions, was assumed. Prediction of the discomfort level, determined by vibrations transmitted from the column to the seat and the body, was examined by taking into account the standard approach [6, 10] applied in vehicle N.V.H. (Noise, Vibration and Harshness) analyses). An analysis of the comfort level in various systems, including all vehicle types, buildings and other structures, is very important and required by certification authorities [9, 16] Many tests have been reported on how the human body perceives the discomfort [8]. It is a common practice to

simulate and test comfort parameters also in special or construction machinery, as, for example, in [3] but especially in many branches of the ground vehicle industry.

**2. Mathematical model of the forest crane**

The model of the forest crane which consists of eight rigid links is presented in Fig. 1. These links are driven by flexible drive models generating drive torques  $\mathbf{t}^{(d,i)}$  and drive force  $\mathbf{f}^{(d,4)}$  The whole crane (its platform) is supported on eight flexible legs. Similarly, mass-less spring damping elements model the connection between the seat and the crane's column.

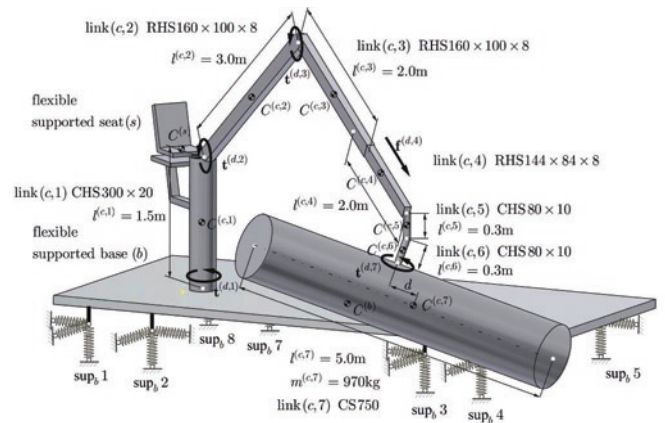


Fig. 1. Model of the forest crane

Joint coordinates and homogeneous transformation matrices are used to describe the geometry of the forest crane. The local coordinate systems and numeration of certain points are shown in Fig. 2.

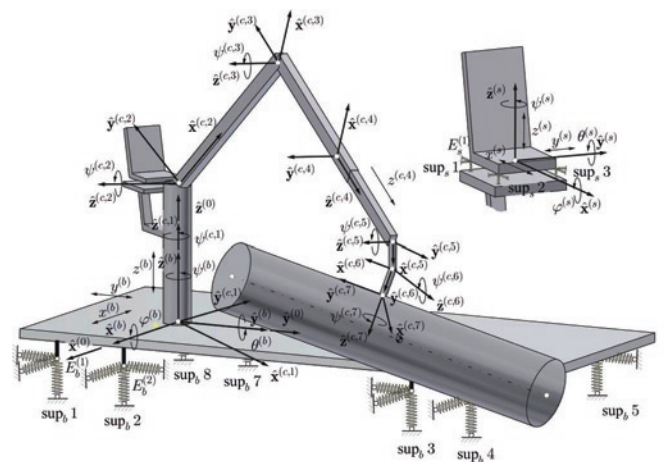


Fig. 2. Coordinate systems and notation applied to crane links

The vector of the model's generalised coordinates has the following form:

$$\mathbf{q} = (q_k)_{k=1, \dots, n_{dof}} = \left[ \left( \mathbf{q}^{(b)} \right)^T \quad \left( \mathbf{q}^{(c)} \right)^T \quad \left( \mathbf{q}^{(s)} \right)^T \right]^T \quad (1)$$

where:

$$\mathbf{q}^{(b)} = (q_j^{(b)})_{j=1, \dots, 6} = \left[ x^{(b)} \quad y^{(b)} \quad z^{(b)} \quad \psi^{(b)} \quad \theta^{(b)} \quad \varphi^{(b)} \right]^T$$

$$\mathbf{q}^{(c)} = (q_j^{(c)})_{j=1, \dots, 7} = \left[ \psi^{(c,1)} \quad \psi^{(c,2)} \quad \psi^{(c,3)} \quad z^{(c,4)} \quad \psi^{(c,5)} \quad \psi^{(c,6)} \quad \psi^{(c,7)} \right]^T$$

$$\mathbf{q}^{(s)} = (q_j^{(s)})_{j=1, \dots, 6} = \left[ x^{(s)} \quad y^{(s)} \quad z^{(s)} \quad \psi^{(s)} \quad \theta^{(s)} \quad \varphi^{(s)} \right]^T$$

The homogeneous transformation matrices have the following forms:

$$\mathbf{T}_{\alpha \in \{b,s\}}^{(\alpha)} = \begin{bmatrix} c\psi^{(\alpha)}c\theta^{(\alpha)} & c\psi^{(\alpha)}s\theta^{(\alpha)}s\varphi^{(\alpha)} - s\psi^{(\alpha)}c\varphi^{(\alpha)} & c\psi^{(\alpha)}s\theta^{(\alpha)}c\varphi^{(\alpha)} + s\psi^{(\alpha)}s\varphi^{(\alpha)} & x^{(\alpha)} \\ s\psi^{(\alpha)}c\theta^{(\alpha)} & s\psi^{(\alpha)}s\theta^{(\alpha)}s\varphi^{(\alpha)} + c\psi^{(\alpha)}c\varphi^{(\alpha)} & s\psi^{(\alpha)}s\theta^{(\alpha)}c\varphi^{(\alpha)} - c\psi^{(\alpha)}s\varphi^{(\alpha)} & y^{(\alpha)} \\ -s\theta^{(\alpha)} & c\theta^{(\alpha)}s\varphi^{(\alpha)} & c\theta^{(\alpha)}c\varphi^{(\alpha)} & z^{(\alpha)} \\ 0 & 0 & 0 & 1 \end{bmatrix}$$

$$\tilde{\mathbf{T}}^{(c,1)} = \begin{bmatrix} c\psi^{(c,1)} & -s\psi^{(c,1)} & 0 & 0 \\ s\psi^{(c,1)} & c\psi^{(c,1)} & 0 & 0 \\ 0 & 0 & 1 & 0 \\ 0 & 0 & 0 & 1 \end{bmatrix}, \quad \tilde{\mathbf{T}}^{(c,2)} = \begin{bmatrix} c\psi^{(c,2)} & -s\psi^{(c,2)} & 0 & 0 \\ 0 & 0 & -1 & 0 \\ s\psi^{(c,2)} & c\psi^{(c,2)} & 0 & l^{(c,1)} \\ 0 & 0 & 0 & 1 \end{bmatrix},$$

$$\tilde{\mathbf{T}}^{(c,3)} = \begin{bmatrix} c\psi^{(c,3)} & -s\psi^{(c,3)} & 0 & l^{(c,2)} \\ s\psi^{(c,3)} & c\psi^{(c,3)} & 0 & 0 \\ 0 & 0 & 1 & 0 \\ 0 & 0 & 0 & 1 \end{bmatrix}, \quad \tilde{\mathbf{T}}^{(c,4)} = \begin{bmatrix} 1 & 0 & 0 & 0 \\ 0 & 0 & -1 & -z^{(c,4)} \\ 0 & 1 & 0 & 0 \\ 0 & 0 & 0 & 1 \end{bmatrix},$$

$$\tilde{\mathbf{T}}^{(c,5)} = \begin{bmatrix} c\psi^{(c,5)} & -s\psi^{(c,5)} & 0 & 0 \\ 0 & 0 & 1 & 0 \\ -s\psi^{(c,5)} & -c\psi^{(c,5)} & 0 & 0 \\ 0 & 0 & 0 & 1 \end{bmatrix}, \quad \tilde{\mathbf{T}}^{(c,6)} = \begin{bmatrix} c\psi^{(c,6)} & -s\psi^{(c,6)} & 0 & l^{(c,5)} \\ 0 & 0 & 1 & 0 \\ -s\psi^{(c,6)} & -c\psi^{(c,6)} & 0 & 0 \\ 0 & 0 & 0 & 1 \end{bmatrix},$$

$$\tilde{\mathbf{T}}^{(c,7)} = \begin{bmatrix} c\psi^{(c,7)} & -s\psi^{(c,7)} & 0 & 0 \\ 0 & 0 & 1 & l^{(c,6)} \\ -s\psi^{(c,7)} & -c\psi^{(c,7)} & 0 & 0 \\ 0 & 0 & 0 & 1 \end{bmatrix}, \quad s\alpha^{(\beta)} = \sin\alpha^{(\beta)}, \quad c\alpha^{(\beta)} = \cos\alpha^{(\beta)}.$$

The equations of motion are derived using Lagrange equations of the second order. The following general form is commonly used:

$$\dot{\mathbf{z}}^{(j)} = \mathbf{LuGre}(t, \mathbf{q}^{(c)}, \mathbf{z}^{(j)}) \quad (2.1)$$

$$\mathbf{M}\mathbf{q} = \mathbf{e}(t, \mathbf{q}, \dot{\mathbf{q}}) + \mathbf{s}(\mathbf{q}, \dot{\mathbf{q}}) + \mathbf{d}(t, \mathbf{q}^{(c)}, \dot{\mathbf{q}}^{(c)}) - \mathbf{f}(t, \mathbf{q}^{(c)}, \dot{\mathbf{q}}^{(c)}) \quad (2.2)$$

where:

$$(\mathbf{LuGre})_{i=1, \dots, 7} = \dot{q}_i^{(c)} \left( 1 - \frac{\sigma_{0,i}^{(j)} z_i^{(j)} \operatorname{sgn}(\dot{q}_i^{(c)})}{\mu_{k,i}^{(j)} + \left( \mu_{s,i}^{(j)} - \mu_{k,i}^{(j)} \right) \exp\left( -\left( \frac{\dot{q}_i^{(c)}}{\dot{q}_{S,i}^{(c)}} \right)^2 \right)} \right)$$

$$\boldsymbol{\mu}^{(j)} = \sigma_0^{(j)} \mathbf{z}^{(j)} + \sigma_1^{(j)} \dot{\mathbf{z}}^{(j)} + \sigma_2^{(j)} \mathbf{q}^{(c)}$$

$$\mathbf{M} = \sum_{\alpha \in \{b,c,s\}} \mathbf{M}^{(\alpha)}$$

$$\mathbf{M}^{(b)} = \begin{bmatrix} \mathbf{M}_{1,1}^{(b)} & 0 \\ 0 & 0 \end{bmatrix}, \quad \mathbf{M}^{(c)} = \begin{bmatrix} \mathbf{M}_{1,1}^{(c)} & \dots & \mathbf{M}_{1,j}^{(c)} & \dots & \mathbf{M}_{1,n_b-1}^{(c)} & 0 \\ \vdots & \ddots & \vdots & \ddots & \vdots & \vdots \\ \mathbf{M}_{i,1}^{(c)} & \dots & \mathbf{M}_{i,j}^{(c)} & \dots & \mathbf{M}_{i,n_b-1}^{(c)} & 0 \\ \vdots & \ddots & \vdots & \ddots & \vdots & \vdots \\ \mathbf{M}_{n_b-1,1}^{(c)} & \dots & \mathbf{M}_{n_b-1,j}^{(c)} & \dots & \mathbf{M}_{n_b-1,n_b-1}^{(c)} & 0 \\ 0 & \dots & 0 & \dots & 0 & 0 \end{bmatrix}$$

$$\mathbf{M}^{(s)} = \begin{bmatrix} 0 & 0 \\ 0 & \mathbf{M}_{1,1}^{(s)} \end{bmatrix}$$

$$\mathbf{M}_{1,1}^{(\alpha)} \Big|_{\alpha \in \{b,s\}} = \left( m_{i,j}^{(\alpha)} \right)_{i,j=1, \dots, n_{dof}^{(\alpha)}}, \quad m_{i,j}^{(\alpha)} = \operatorname{tr} \left\{ \mathbf{T}_i^{(\alpha)} \mathbf{H}^{(\alpha)} \left( \mathbf{T}_j^{(\alpha)} \right)^T \right\},$$

$$\mathbf{M}_{i,j}^{(c)} = \sum_{l=\max\{i,j\}}^{n_b-1} \mathbf{M}_{i,j}^{(c,l)}, \quad m_{i,j}^{(c,l)} = \operatorname{tr} \left\{ \mathbf{T}_i^{(c,l)} \mathbf{H}^{(c,l)} \left( \mathbf{T}_j^{(c,l)} \right)^T \right\},$$

$$\mathbf{e} = \sum_{\alpha \in \{b,c,s\}} \mathbf{e}^{(\alpha)}$$

$$\mathbf{e}^{(b)} = \begin{bmatrix} \mathbf{e}_1^{(b)} \\ 0 \end{bmatrix}, \quad \mathbf{e}^{(c)} = \begin{bmatrix} \mathbf{e}_1^{(c)} \\ \vdots \\ \mathbf{e}_{n_b-1}^{(c)} \\ 0 \end{bmatrix}, \quad \mathbf{e}^{(s)} = \begin{bmatrix} 0 \\ \mathbf{e}_1^{(s)} \end{bmatrix},$$

$$\mathbf{e}_1^{(\alpha)} \Big|_{\alpha \in \{b,s\}} = -\left( \mathbf{h}^{(\alpha)} + \mathbf{g}^{(\alpha)} \right),$$

$$\mathbf{h}^{(\alpha)} = \left( h_i^{(\alpha)} \right)_{i=1, \dots, n_{dof}^{(\alpha)}},$$

$$h_i^{(\alpha)} = \sum_{m=1}^{n_{dof}^{(\alpha)}} \sum_{n=1}^{n_{dof}^{(\alpha)}} \operatorname{tr} \left\{ \mathbf{T}_i^{(\alpha)} \mathbf{H}^{(\alpha)} \left( \mathbf{T}_{m,n}^{(\alpha)} \right)^T \right\} \dot{q}_m^{(\alpha)} \dot{q}_n^{(\alpha)},$$

$$\mathbf{g}^{(\alpha)} = \left( g_i^{(\alpha)} \right)_{i=1, \dots, n_{dof}^{(\alpha)}}, \quad g_i^{(\alpha)} = m^{(\alpha)} g_{i3} \mathbf{T}_i^{(\alpha)} \mathbf{r}_{C^{(\alpha)}}^{(\alpha)},$$

$$\mathbf{e}_i^{(c)} = -\sum_{l=i}^{n_b-1} \left( \mathbf{h}_i^{(c,l)} + \mathbf{g}_i^{(c,l)} \right),$$

$$\mathbf{h}_i^{(c,l)} = \left( h_{n_{dof}^{(c,i-1)} + k}^{(c,l)} \right)_{k=1, \dots, n_{dof}^{(c,i)}},$$

$$h_i^{(c,l)} = \sum_{m=1}^{n_{dof}^{(c,l)}} \sum_{n=1}^{n_{dof}^{(c,l)}} \text{tr} \left\{ \mathbf{T}_i^{(c,l)} \mathbf{H}^{(c,l)} \left( \mathbf{T}_{m,n}^{(c,l)} \right)^T \right\} \dot{q}_m^{(c,l)} \dot{q}_n^{(c,l)},$$

$$\mathbf{g}_i^{(c,l)} = \left( \mathbf{g}_{n_{dof}^{(c,l-1)}+k}^{(c,l)} \right)_{k=1, \dots, n_{dof}^{(c,l)}}, \quad \mathbf{g}_i^{(c,l)} = m^{(c,l)} \mathbf{g} \mathbf{j}_3 \mathbf{T}_i^{(c,l)} \mathbf{r}_{C^{(c,l)}},$$

$$\mathbf{s} = \sum_{\alpha \in \{b,s\}} \mathbf{s}^{(sup_\alpha)}, \quad \mathbf{s}^{(sup_\alpha)} = \left( s_k^{(sup_\alpha)} \right)_{k=1, \dots, n_{nof}},$$

$$s_k^{(sup_b)} = \begin{cases} - \sum_{i=1}^{n_{sup_b}} \left( \frac{\partial \mathbf{e}^{(sup_b,i)}}{\partial q_k} \right)^T \mathbf{S}^{(sup_b,i)} \mathbf{e}^{(sup_b,i)} + \left( \frac{\partial \dot{\mathbf{e}}^{(sup_b,i)}}{\partial \dot{q}_k} \right)^T \mathbf{D}^{(sup_b,i)} \dot{\mathbf{e}}^{(sup_b,i)} & \text{if } q_k \in \{ \mathbf{q}^{(b)} \} \\ 0 & \text{otherwise} \end{cases}$$

$$s_k^{(sup_s)} = \begin{cases} \sum_{i=1}^{n_{sup_s}} \left( \frac{\partial \mathbf{e}^{(sup_s,i)}}{\partial q_k} \right)^T \mathbf{S}^{(sup_s,i)} \mathbf{e}^{(sup_s,i)} + \left( \frac{\partial \dot{\mathbf{e}}^{(sup_s,i)}}{\partial \dot{q}_k} \right)^T \mathbf{D}^{(sup_s,i)} \dot{\mathbf{e}}^{(sup_s,i)} & \text{if } q_k \in \{ \mathbf{q}^{(b)}, \psi^{(c,1)} \} \\ - \sum_{i=1}^{n_{sup_s}} \left( \frac{\partial \mathbf{e}^{(sup_s,i)}}{\partial q_k} \right)^T \mathbf{S}^{(sup_s,i)} \mathbf{e}^{(sup_s,i)} + \left( \frac{\partial \dot{\mathbf{e}}^{(sup_s,i)}}{\partial \dot{q}_k} \right)^T \mathbf{D}^{(sup_s,i)} \dot{\mathbf{e}}^{(sup_s,i)} & \text{if } q_k \in \{ \mathbf{q}^{(s)} \} \\ 0 & \text{otherwise} \end{cases}$$

Based on the formulation presented above, a computer program was developed using the Visual C++ environment. The standard Runge-Kutta method of the fourth order was applied, with a constant time step  $10^{-4}$  s .

**3.1. Crane operation scenarios and load cases**

The crane motion sequence is assumed as presented in Fig. 3. At time  $t = 0$ s the load is resting on a platform. After two seconds, the load is lifted up by increasing angle of the jib. Then crane column rotates (reaching  $90^\circ$  at  $t = 5$ s), and simultaneously the telescopic motion begins at time  $t = 5$ s. For the final column rotation angle,  $\psi_{dr}^{(c,1)} = 180^\circ$ , the telescopic motion stops reaching minimum length at  $t = 9$ s and the cycle finishes with the load positioned down to a platform on the opposite side.

Crane loading conditions are:

- 1) empty grab (  $E$  ) - operation with unloaded crane,
- 2) crane with load (  $F$  ) - operation with  $m^{(c,7)}$  load mass.

The empty load case scenario is considered to have identical driving functions, with reverse order/values - returning to the pick-up position same as in  $t = 0$ s .

As indicated in Fig. 1, the distance  $d$  represents offset between the load's center of gravity and axis of the joint and drive  $\mathbf{t}^{(d,7)}$ . Influence of this distance was considered as one of important parameters in the analysis. Each working cycle, in practical condition, will

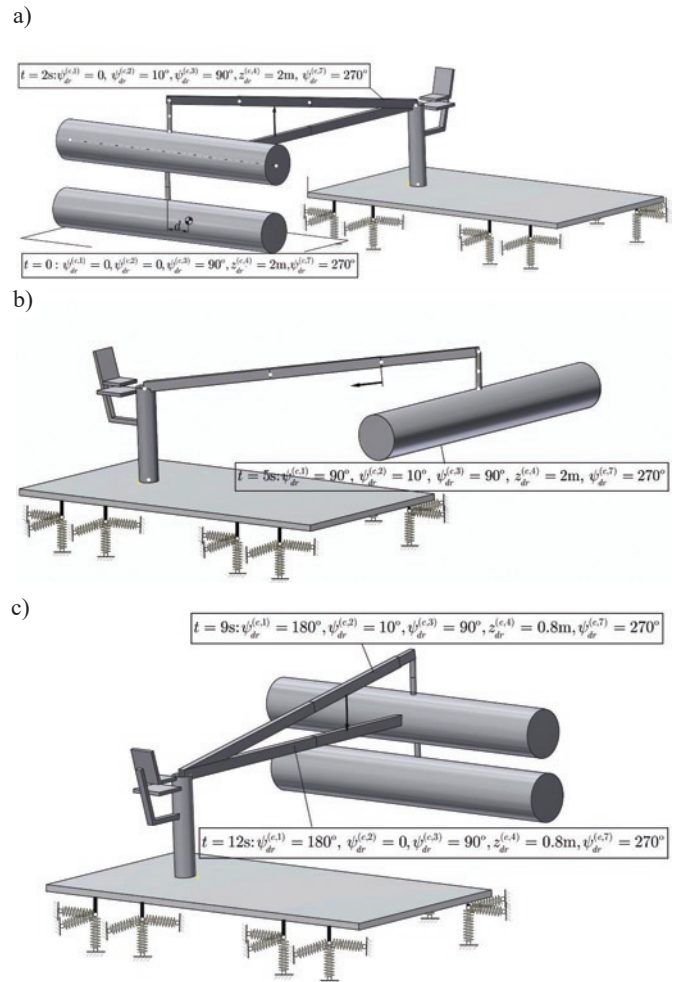


Fig. 3. Crane operation sequences

be characterized by different value of  $d$ , caused by not ideal mass distribution of trunks and misalignment of length, initial position of the load on a storage platform an many other reasons. For the performed study presented in this work, the range of  $d = \pm 20$ cm is assumed as typical.

Load cases analyzed in this work are listed in Fig. 4. „Empty” crane cases are defined for the same sequence as loaded - just with no load attached to the grab. „Loaded” cases are performed with the tree trunk mass  $m^{(c,7)} = 970$ kg .

$$\begin{array}{l} x = 0 \text{ (no damping)} \\ x = 1 \text{ (nominal damping)} \end{array} \left| \begin{array}{l} L = F \text{ (loaded crane)} \\ L = E \text{ (empty hook)} \end{array} \right.$$

$$Dx - Fy - dz - L$$

$$\begin{array}{l} y = 1 \text{ (friction coeffs. "Set-1")} \\ y = 2 \text{ (friction coeffs. "Set-2")} \end{array} \left\{ \begin{array}{l} z = 0 \text{ (no load CoG offset)} \\ z = 10 \text{ (10cm offset of load CoG)} \\ z = 20 \text{ (20cm offset of load CoG)} \end{array} \right.$$

Fig. 4. Analyzed cases and symbol assignation

The cases without damping in seat mounts are analyzed just for comparison of the damping effect on operator vibration level. Analysis of all possible cases, leading to a more general evaluation of the particular crane design, is a large task and will not be presented in details.

**3.2. Main parameters of the system**

All the crane mass components have assigned properties according to geometry properties (sections) as indicated in Fig. 1. Operator's seat mass is assumed as a combined mass of the operator (one single

Table 1. Parameters of the crane supports

	1	2	3	4	5	6	7	8
$x_{E_b^{(i)}}^{(b)}$ [m]	1.5	1.5	1.5	1.5	-1.5	-1.5	-1.5	-1.5
$y_{E_b^{(i)}}^{(b)}$ [m]	0	1.0	8.0	9.0	9.0	8.0	1.0	0
$z_{E_b^{(i)}}^{(b)}$ [m]					-0.57			
$s_{\alpha}^{(sup_b, i)} \Big _{\alpha \in \{x, y\}}$ [Nm <sup>-1</sup> ]					3 · 10 <sup>6</sup>			
$s_Z^{(sup_b, i)}$ [Nm <sup>-1</sup> ]					1 · 10 <sup>7</sup>			
$d_{\alpha}^{(sup_b, i)} \Big _{\alpha \in \{x, y\}}$ [Nsm <sup>-1</sup> ]					5 · 10 <sup>4</sup>			
$d_Z^{(sup_b, i)}$ [Nsm <sup>-1</sup> ]					9 · 10 <sup>4</sup>			

Table 2. Parameters of the seat supporting elements

	1	2	3	4
$x_{E_s^{(i)}}^{(s)}$ [m]	-0.25	0.25	0.25	-0.25
$y_{E_s^{(i)}}^{(s)}$ [m]	0.25	0.25	-0.25	-0.25
$z_{E_s^{(i)}}^{(s)}$ [m]			-0.05	
$x_{E_s^{(i)}}^{(c, 1)}$ [m]	-0.85	-0.35	-0.35	-0.85
$y_{E_s^{(i)}}^{(c, 1)}$ [m]	0.25	0.25	-0.25	-0.25
$z_{E_s^{(i)}}^{(c, 1)}$ [m]			1.4	
$s_{\alpha}^{(sup_s, i)} \Big _{\alpha \in \{x, y\}}$ [Nm <sup>-1</sup> ]			10 <sup>3</sup>	
$s_Z^{(sup_s, i)}$ [Nm <sup>-1</sup> ]			9 · 10 <sup>3</sup>	
$d_{\alpha}^{(sup_s, i)} \Big _{\alpha \in \{x, y\}}$ [Nsm <sup>-1</sup> ]			40	
$d_Z^{(sup_s, i)}$ [Nsm <sup>-1</sup> ]			120	

Table 3. Friction parameters

		1	2	3	4	5	6	7
Set-1	$\mu_{k,i}^{(j)}$	0.15	0.10	0.10	0.10	0.15	0.15	0.15
	$\mu_{s,i}^{(j)}$	0.20	0.15	0.20	0.20	0.20	0.20	0.20
Set-2	$\mu_{k,i}^{(j)}$	0.07	0.07	0.05	0.20	0.20	0.20	0.10
	$\mu_{s,i}^{(j)}$	0.10	0.10	0.15	0.30	0.35	0.35	0.15
	$\dot{q}_{S,i}^{(c)} [\text{rad s}^{-1}, \text{ms}^{-1}]$				0.005			
	$\sigma_{0,i}^{(j)} [\text{Nmrad}^{-1}, \text{Nm}^{-1}]$		$10^5$		$10^7$		$10^5$	
	$\sigma_{1,i}^{(j)} [\text{Nmsrad}^{-1}, \text{Nsm}^{-1}]$				5			
	$\sigma_{2,i}^{(j)} [\text{Nmsrad}^{-1}, \text{Nsm}^{-1}]$				0			

mass 80kg) and the seat self-mass equal to 25kg; hence the total mass of the seat-operator is assumed to be  $m^{(s)} = 105\text{kg}$ .

The geometrical parameters of the base supports are contained in Tab.1. The assumed stiffness and damping coefficients are also presented. The mounting point locations and spring-damping elements connecting the crane column and seat body are specified as presented in Tab. 2. The friction parameters are defined in Tab. 3. Two sets are defined in order to distinguish different conditions of the joints, i.e. normal (Set-1) well lubricated, and poorly greased joints (Set-2).

3.3. Vibration assessment

Human perception of discomfort is not unique to every person, i.e. perceived comfort depends on many factors. The reference standards used in the industry are, e.g. BS 6841 and ISO 2631-1 – Fig. 5. These standards were used in this work to assess the level of vibration and discomfort as perceived by the operator. A similar approach can be applied for vehicle dynamics and an estimation of the ride comfort, which was also applied in the optimisation routines yielding the desired minimum discomfort [31].

In general, the body is exposed to vibration in combination of all 6 directions (translations and rotations), but in present work only  $x, y, z$  axial signals are considered. Seated crane operator will perceive vibration at the back and at the feet (as well as hands and the head may also be of importance). The assigned locations investigated and appropriate filters are indicated in Fig. 6.

Each considered location for comfort evaluation is characterized by the following formulas:

$$PV_{RMS}^{(\alpha)} \Big|_{\alpha \in \{O_b, O_s, O_f\}} = \sqrt{\sum_{\beta \in \{x,y,z\}} \left( f_{\beta}^{(\alpha)} RMS_{\beta}^{(\alpha)} \right)^2}, \quad (3.1)$$

$$PV_{VDV}^{(\alpha)} \Big|_{\alpha \in \{O_b, O_s, O_f\}} = 4 \sqrt{\sum_{\beta \in \{x,y,z\}} \left( f_{\beta}^{(\alpha)} VDV_{\beta}^{(\alpha)} \right)^4}. \quad (3.2)$$

A single values describing comfort level for the whole construction, are defined as the sum of all location values. Proposed approach will enable us to summarize the comfort as one single values, which can be compared between different designs or different operations. The following definitions apply:

$$SV_{RMS}^{(c)} = \sqrt{\sum_{\alpha \in \{O_b, O_s, O_f\}} \left( PV_{RMS}^{(\alpha)} \right)^2}, \quad (3.3)$$

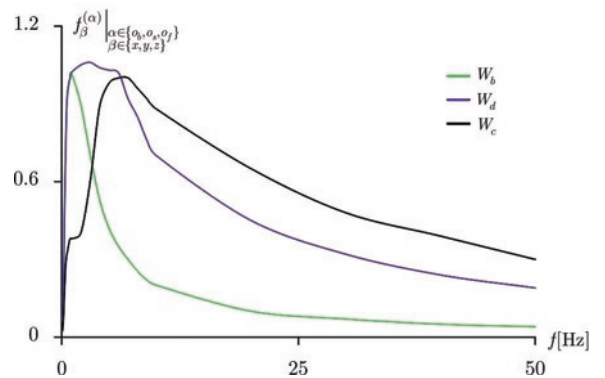


Fig. 5. Frequency-weighting filters to be applied in comfort assessment

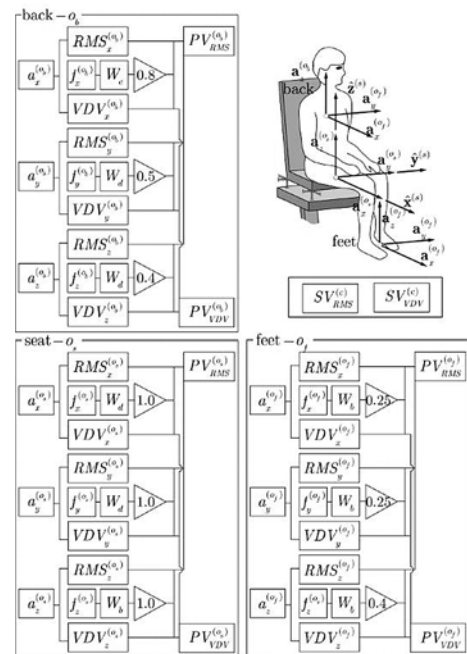


Fig. 6. Locations of interest and frequency-weighting filters

$$SV_{VDV}^{(c)} = \sqrt{\sum_{\alpha \in \{O_b, O_s, O_f\}} \left( PV_{VDV}^{(\alpha)} \right)^2}. \quad (3.4)$$

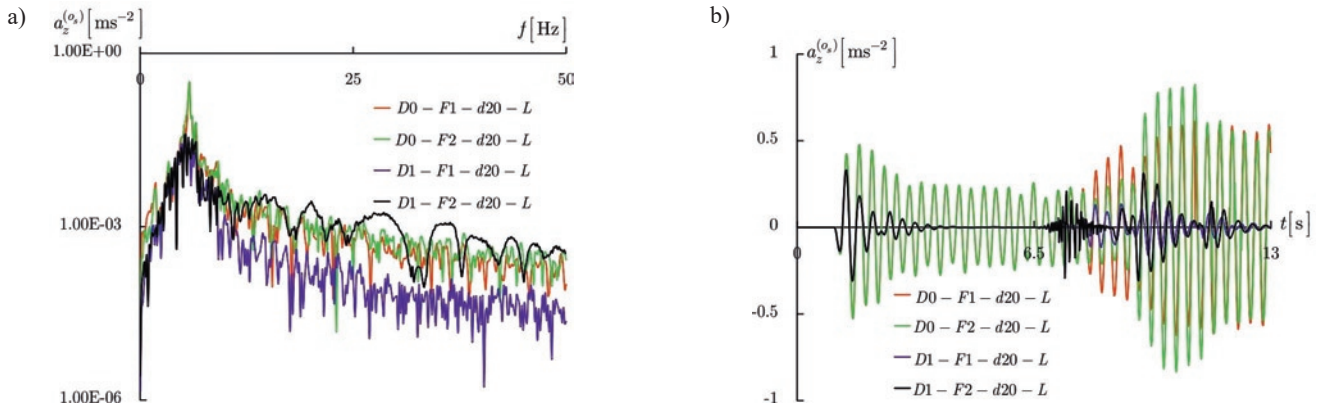


Fig. 7. Accelerations calculated for seat position in  $z$  direction; loaded crane with and without damping in seat mount elements. Frequency plots are on the left; time histories are on the right.

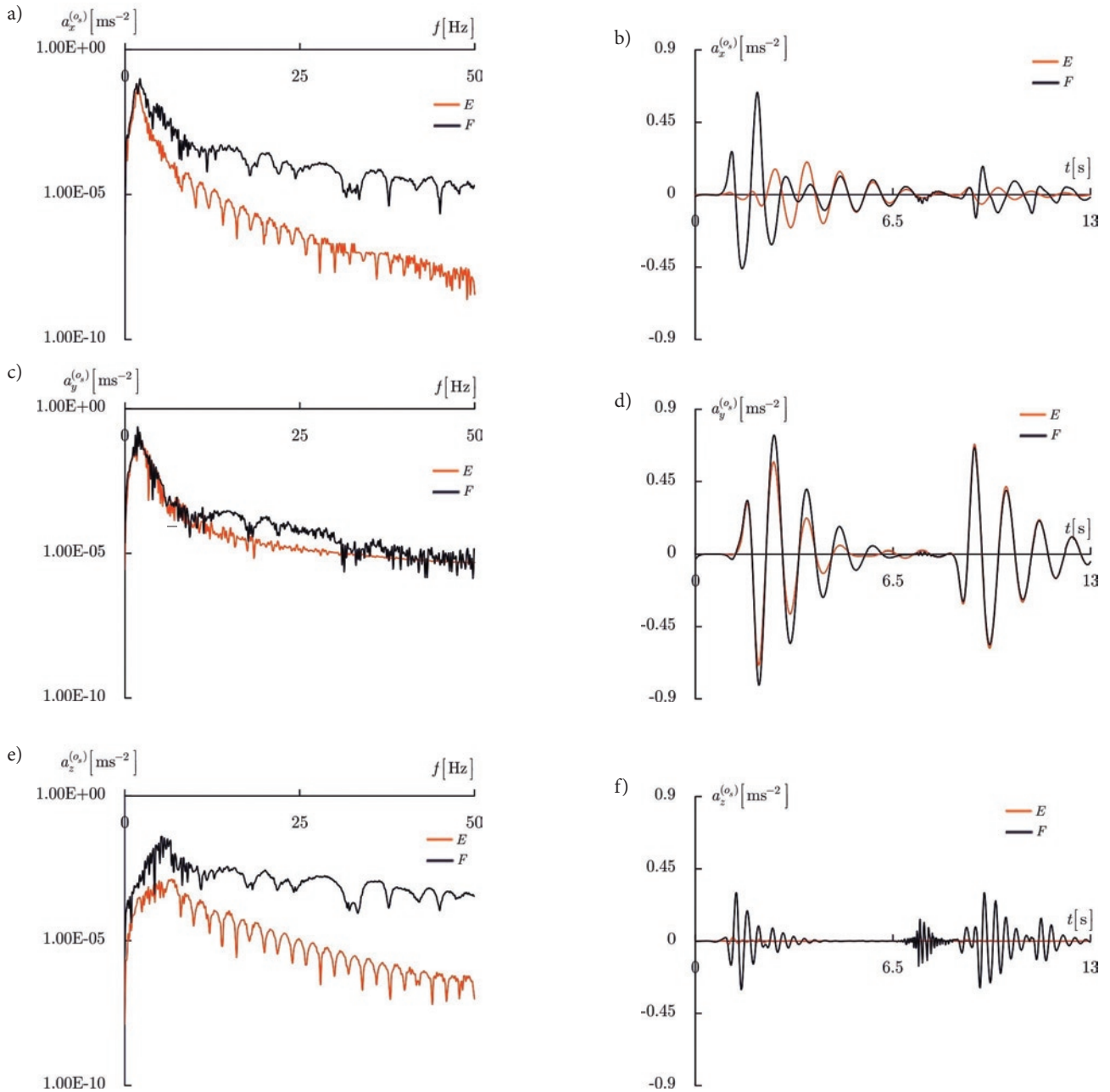


Fig. 8. Accelerations (filtered) calculated for seat position in  $x, y, z$  direction operation; with empty and loaded crane (load cases  $D1 - F2 - d0 - E$  and  $D1 - F2 - d20 - F$ ). Frequency (filtered) plots on the left; time histories on right.

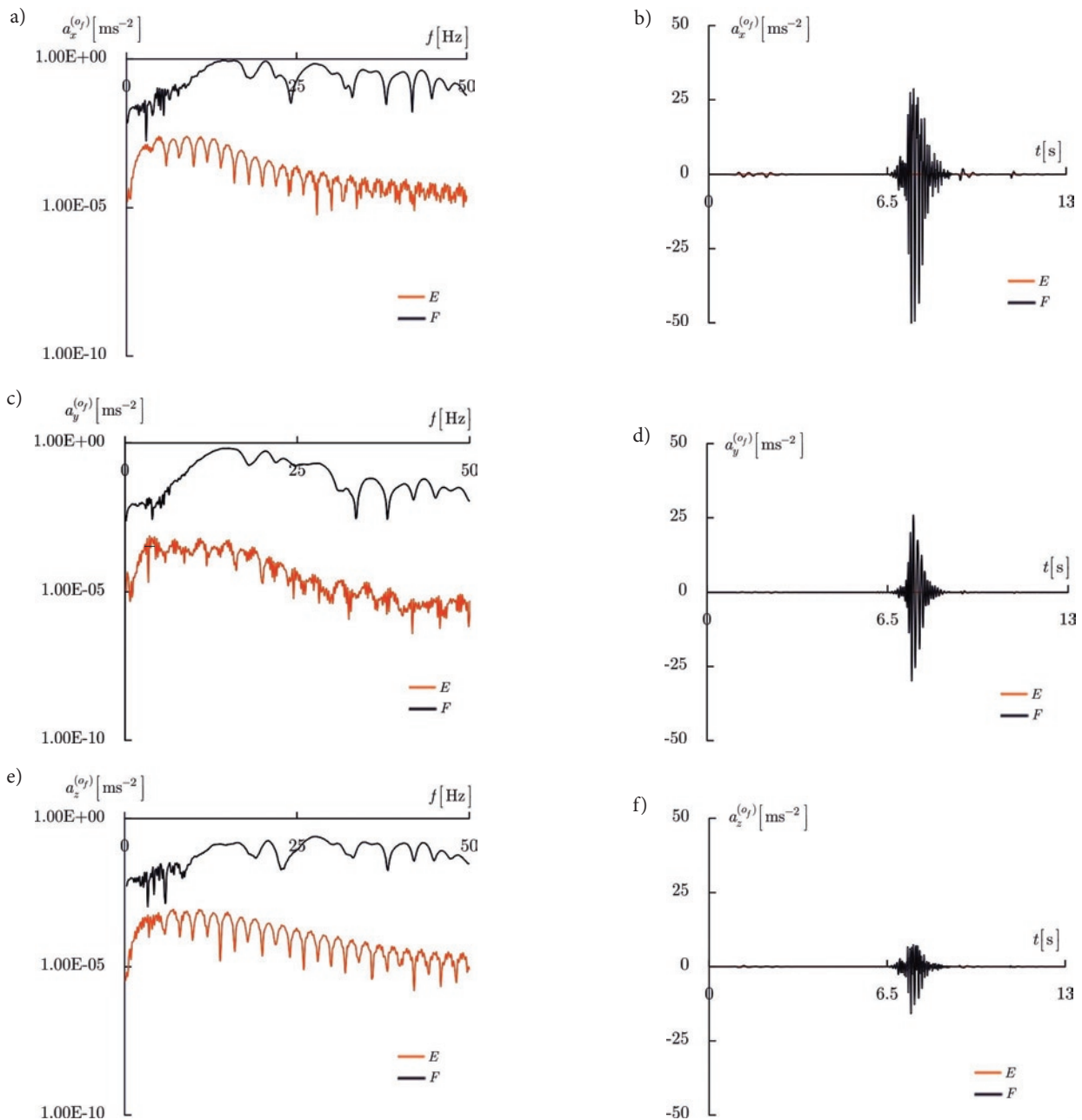


Fig. 9. Accelerations (filtered) calculated for feet rest position in  $x, y, z$  direction; operation with empty and loaded crane (load cases  $D1 - F2 - d0 - E$  and  $D1 - F2 - d20 - F$ ). Frequency (filtered) plots on the left; time histories on the right.

Other definitions (such as the „running RMS” (BS 6841) and peak-to-peak could also have been applied to assess the effect on vibration discomfort [3]. The selection of most appropriate parameter will be of designer choice and should be done based on type of operation performed by the crane. This could yield to the optimization routines resulting in minimization of the discomfort, but changing for example the mount characteristics or locations of the support points.

## 4. Simulation results

### 4.1. Example time histories

Some example results are shown in Fig. 7 – all series show the time histories and frequencies calculated for the vertical acceleration

of the seat (unfiltered results are shown). The damping effect on the seat mounting points is examined. Typically, accelerations for the system without damping would be too conservative, even if a simple seat system for some poor designs may not have any damping elements (only structural damping).

Accelerations calculated for friction parameters Set-2 and for empty hook operation (unloaded crane) are presented in Fig. 8. A similar set of results for the feet rest is presented in Fig. 9. The friction effect on the transnational motion of the jib (drive activated during rotation) is well evident on the feet.

The influence of the load centre of gravity ( $d = 0\text{cm}$ ,  $d = 10\text{cm}$ ,  $d = 20\text{cm}$ ) is presented in Fig. 10. The results show the strong influence of the load centre of gravity (and induced moments) on crane dynamics. A high friction force is generated in the jib (during the telescopic phase of motion) and the peaks are strongly visible. Most of

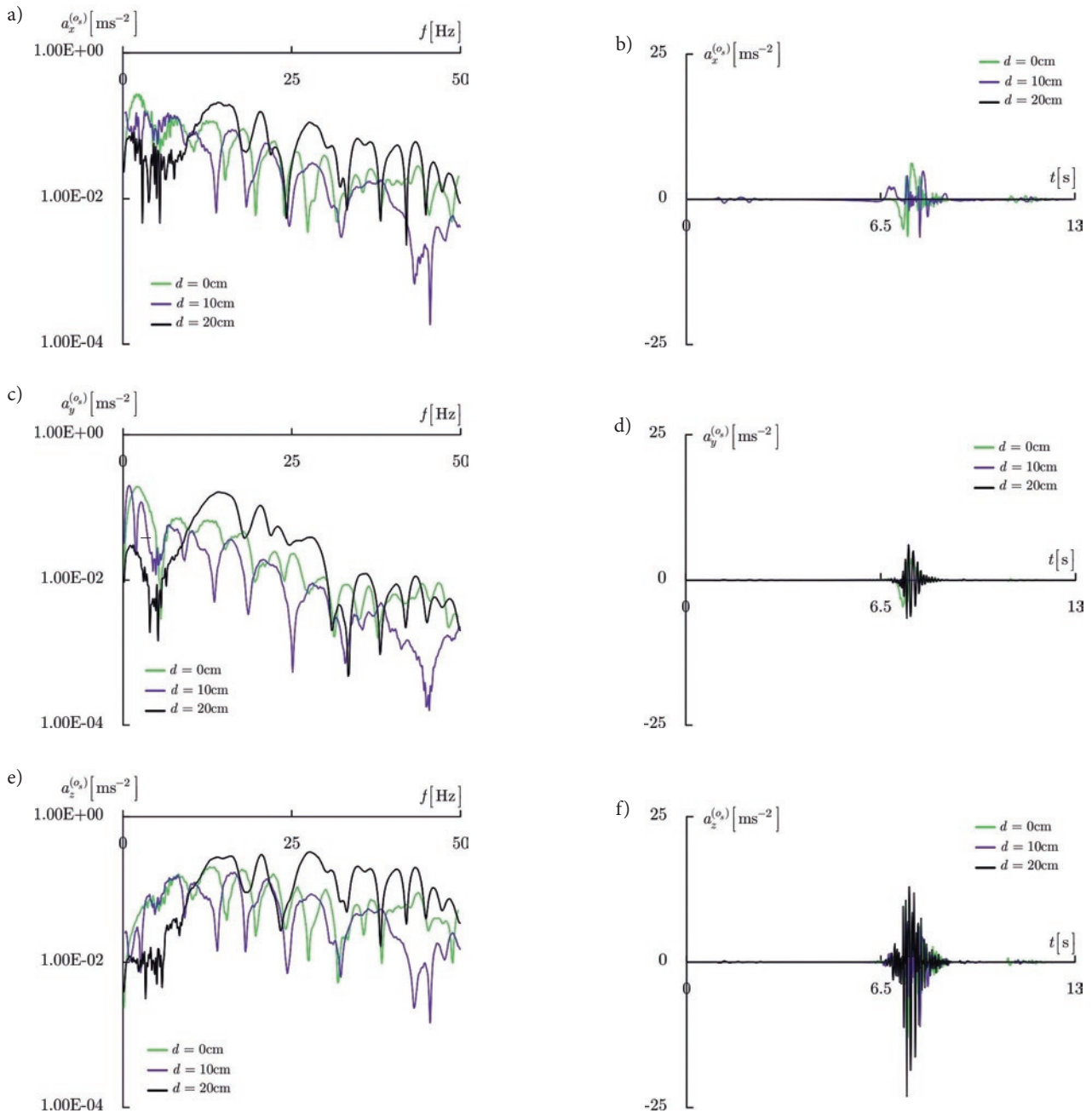


Fig. 10. Accelerations (filtered) calculated for seat base position in  $x, y, z$  direction; operation with loaded crane and different  $d$  value. Frequency (filtered) plots are on the left; time histories are on the right. Load cases:  $D1-F2-d0-F$ ,  $D1-F2-d10-F$  and  $D1-F2-d20-F$

these peaks are transferred to the feet floor and seat base. Seat suspension, however, provides good isolation and the peaks visible between 6÷9 s are not reflected in the seat points (such as the seat and backrest).

**4.2. Vibration level - indexes**

Various indexes related to perceived discomfort are shown in this section for the analysed crane operation scenarios.

Some indexes for load scenarios and design parameters listed in section 3.2 and 3.1 are presented in Tab. 6. Calculations have been performed with friction set **Set-2** (case  $D1-F2-d0-E$ ).

Similarly, the results for crane handling with a full load considering two different friction coefficient sets **Set-1** and **Set-2** are listed in Tab. 7 and Tab. 8.

Some parameters defined in section 3.3, calculated for assumed friction parameters in crane joint as defined by **Set-1** and **Set-2** are presented in Fig. 11. Filtered  $RMS$  values, reduced to one single value,  $SV_{RMS}^{(e)}$ , are shown (calculated as indicated in Fig. 6). Results are calculated for the whole crane seat comfort when the seat suspension is included. For comparison, the results indicate also the level of  $RMS$  when rigid support would be assumed.

The time (in hours for **Set-1** and minutes for **Set-2**) required to accumulate desired level of dose value (i.e.  $15ms^{-1.75}$ ) is indicated

Table 6. Vibration discomfort parameters, case D2-F2-d0-E

Parameter	rigid seat			flexible seat			back			feet		
	<i>x</i>	<i>y</i>	<i>z</i>	<i>x</i>	<i>y</i>	<i>z</i>	<i>x</i>	<i>y</i>	<i>z</i>	<i>x</i>	<i>y</i>	<i>z</i>
<i>RMS</i>	0.01	0.00	0.00	0.06	0.21	0.00	0.07	0.22	0.00	0.01	0.00	0.00
<i>PV<sub>RMS</sub></i>		0.01			0.22			0.12			0.00	
<i>SV<sub>RMS</sub></i>					0.25							
<i>RMQ</i>	0.01	0.00	0.01	0.10	0.32	0.01	0.10	0.33	0.01	0.03	0.01	0.01
<i>VDV</i>	0.02	0.00	0.01	0.19	0.61	0.01	0.20	0.63	0.01	0.05	0.01	0.02
<i>PV<sub>VDV</sub></i>		0.02			0.61			0.63			0.05	
<i>K</i>	20.51	12.68	62.06	5.44	5.21	20.25	5.44	5.03	5.68	54.81	24.95	68.61
<i>C<sub>f</sub></i>	6.90	5.32	11.66	3.21	3.28	6.99	3.20	3.18	3.09	10.64	8.37	11.17

Table 7. Vibration discomfort parameters, case D1-F1-d0-F

Parameter	rigid seat			flexible seat			back			feet		
	<i>x</i>	<i>y</i>	<i>z</i>	<i>x</i>	<i>y</i>	<i>z</i>	<i>x</i>	<i>y</i>	<i>z</i>	<i>x</i>	<i>y</i>	<i>z</i>
<i>RMS</i>	0.19	0.04	0.19	0.13	0.24	0.06	0.16	0.25	0.03	0.50	0.09	0.15
<i>PV<sub>RMS</sub></i>		0.27			0.28			0.18			0.14	
<i>SV<sub>RMS</sub></i>					0.36							
<i>RMQ</i>	0.38	0.09	0.47	0.23	0.36	0.10	0.30	0.37	0.06	1.21	0.19	0.35
<i>VDV</i>	0.72	0.17	0.89	0.44	0.68	0.20	0.56	0.70	0.11	2.30	0.36	0.66
<i>PV<sub>VDV</sub></i>		0.97			0.71			0.48			0.58	
<i>K</i>	13.90	20.27	37.11	10.39	4.95	9.98	11.23	4.75	13.14	34.62	22.47	31.63
<i>C<sub>f</sub></i>	6.06	7.10									7.72	9.90

Table 8. Vibration discomfort parameters, case D1-F2-d20-F

Parameter	rigid seat			flexible seat			back			feet		
	<i>x</i>	<i>y</i>	<i>z</i>	<i>x</i>	<i>y</i>	<i>z</i>	<i>x</i>	<i>y</i>	<i>z</i>	<i>x</i>	<i>y</i>	<i>z</i>
<i>RMS</i>	1.04	0.73	2.01	0.13	0.24	0.07	0.17	0.25	0.04	5.11	3.10	1.38
<i>PV<sub>RMS</sub></i>		2.38			0.28			0.18			1.59	
<i>SV<sub>RMS</sub></i>					1.63							
<i>RMQ</i>	1.67	1.07	2.45	0.24	0.37	0.15	0.31	0.37	0.07	6.53	2.28	1.64
<i>VDV</i>	3.18	2.04	4.65	0.45	0.69	0.29	0.59	0.71	0.13	12.39	4.33	3.11
<i>PV<sub>VDV</sub></i>		4.92			0.73			0.51			3.13	
<i>K</i>	29.38	29.10	53.16	11.69	4.88	9.10	12.21	4.69	8.28	64.23	65.46	44.08
<i>C<sub>f</sub></i>	8.91	8.56	11.87	5.10	3.36	4.59	5.47	3.20	4.30	13.02	12.46	11.09

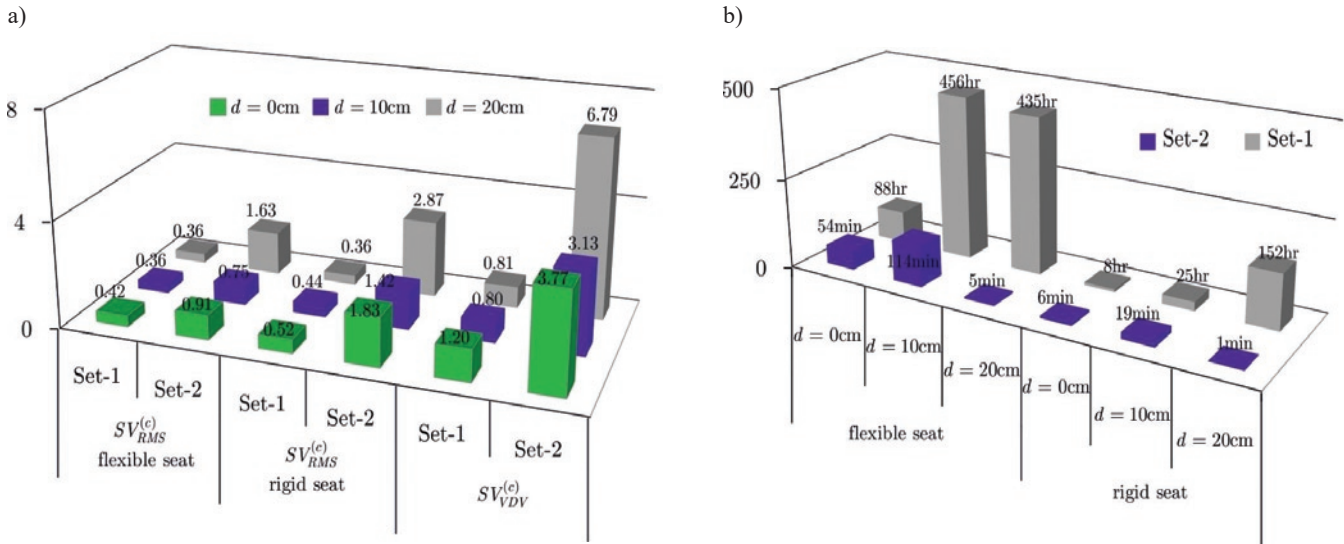


Fig. 11.  $SV_{RMS}^{(c)}$  and  $SV_{VDV}^{(c)}$  values (left),  $T_{15}^{(c)}$  time (right). Loaded crane operation, friction coefficients: **Set-1** and **Set-2**.

in Fig. 11. This is the time calculated considering total vibration dose value from relation:

$$T_{15}^{(c)} = \left( \frac{15}{\sqrt{\sum_{\alpha \in \{O_b, O_s, O_f\}} (VDV_c^{(\alpha)})^2}} \right)^4 t \quad (4.1)$$

where  $t = 13s$ .

For the friction coefficients assumed in **Set-1**, the general level of discomfort can be estimated as “a little uncomfortable” when working with or without dampened seat. Also the exposure time is large, especially for the crane equipped with suspended seat. The values of  $T_{15}^{(c)}$  show much greater difference between isolated and rigid seats. As this measure better suits for the characteristics of signals, it should be more important than the  $SV_{RMS}^{(c)}$  index. Hence, much worse conditions for operator are expected when the seat is rigidly connected to the column. In the worst case, working 8hr in such conditions will be perceived as severe/huge discomfort and potentially dangerous for health.

Different tendency is obtained for **Set-2** friction coefficients: significantly worse results (bigger discomfort) were calculated when handling the trunk with larger offset between the grab axis and its center of gravity ( $d = 20cm$ ). This conditions generated double  $SV_{RMS}^{(c)}$  value and reduced the time  $T_{15}^{(c)}$  to almost minimum (few minutes). For a seat with dampening elements, the RMS at level 0.8÷1.6 can be classified as moderate discomfort, while for the case without such elements (rigid seat), the same operation will lead to very an uncomfortable level.

When considering the duration of such a level of vibration, the operator should not work on the „rigid seat”, when some higher friction would occur. Assuming, that the trunks are not always transported in condition  $d = 20cm$ , but mostly around  $d = (0÷10)cm$ , operator could work on the crane within some limited time 1÷2 hr until the VDV would become unacceptable. Considering the typical use of the forest crane (loading/unloading time is not dominating during the

whole day, typically), estimated results shows how the current machine design could influence on health aspects.

Different results are obtained for operation with unloaded crane; for this conditions the vibrations generated due to operation of empty crane do not cause any significant discomfort for the operator, and the level of friction is also not important (for indexes used in the discomfort assessment). Dominated effect, in the case of unloaded crane, is the motion due to drives, and since there is no load applied (except for the inertia induced forces), the crane operator perceived discomfort is practically identical. The combined value for the seat:  $SV_{RMS}^{(O_s)} = 0.25$  (both friction sets) can be classified as „not uncomfortable”.

Presented results cover only one configuration of the seat suspension. Several iterations are normally performed in order to find a good balance between desired comfort and design constrains.

## 5. Conclusions

The model and computer software developed here were applied to analyse the influence of friction on crane operators. The calculated responses can be useful for designers and early phase design can be examined. The results confirm that high friction can have a significant impact on human discomfort. This parameter, as well as many others, should be taken into account in the initial phase at crane design.

The model presented in this paper can be applied to many other aspects of typical working scenarios. Only the acceleration results are analysed in more detail, but the computer model allows us to investigate much more parameters, such as loads in specific components, the drive function effects on these loads, or optimisation of geometry and stiffness parameters. The model’s simplicity and effectiveness are also important, especially for examining specific aspects of the system when many variant calculations are needed.

More advanced models taking into account, for example, the flexibility of the links can also be the correct direction for more detailed vibration/comfort analyses. This can be addressed in a similar way as presented in this work, i.e. just by extending the model. The disadvantage will be the time required for the analyses and the fact that some more complex input data are required.

## References

1. Augustynek K, Urbaś A. Comparison of bristles' friction models in dynamics analysis of spatial linkages. *Mechanics Research Communications* 2017, <https://doi.org/10.1016/j.mechrescom.2017.01.003>.
2. Åström K J, Canudas-de-Witt C. Revisiting the LuGre model. *IEEE Control Systems Magazine*. Institute of Electrical and Electronics Magazine 2008; 28(6): 101-114, <https://doi.org/10.1109/MCS.2008.929425>.
3. Cann A P, Salmoni A W, Vi P, Eger T R. An exploratory study of whole-body vibration exposure and dose while operating heavy equipment in the construction industry. *Applied Occupational and Environmental Hygiene* 2003; 18: 999-1005, <https://doi.org/10.1080/715717338>.
4. Courtney-Pratt J S, Eisner E. The effect of a tangential force on the contact of metallic bodies. *Proceedings of the Royal Society* 1957; A: 529-550.
5. Craig J J. Introduction to robotics. Mechanics and control. Addison-Wesley Publishing Company, Inc., 1989.
6. BS 6841. Guide to measurement and evaluation of human exposure to whole-body mechanical vibration and repeated shock. British Standard, 1987.
7. Denavit J, Hartenberg R S. A kinematic notation for lower-pair mechanisms based on matrices. *Journal of Applied Mechanics* 1995; 23: 215-221.
8. Giacomini M, Hacaambwa T M. Performance of ISO2631 and BS6841 Comfort Criteria for Evaluating Automobile Road Vibrations, OIA1083, ATA 7th International Conference on the Role of Experimentation in the Modern Automotive Product Development Process, Florence, Italy, May 23-25, 2001.
9. Griffin M J. Handbook of Human Vibration. Elsevier Academic Press, 1990.
10. ISO 2631-1. Mechanical vibration and shock - Evaluation of human exposure to whole body vibration. Part 1: General requirements. International Organization for Standardization, 1997.
11. Jurevič E I (ed.). Dynamics of robot control. Nauka. Moscow: 1984. (in Russian)
12. La Hera P X, Morales D O. Non-linear dynamics modelling description for simulating the behavior of forestry cranes. *International Journal of Modelling Identification and Control* 2014; 21(2): 125-138, <https://doi.org/10.1504/IJMIC.2014.060006>.
13. La Hera P, Morales D O. Model-based development of control systems for forestry cranes. *Journal of Control and Science and Engineering* 2015; ID 256951, <https://doi.org/10.1155/2015/256951>.
14. Legnani G, Casalo F, Righettini P, Zappa B. A homogeneous matrix approach to 3D kinematics and dynamics – I. Theory, Mechanism and Machine Theory 1996; 31(5): 586-605, [https://doi.org/10.1016/0094-114X\(95\)00100-D](https://doi.org/10.1016/0094-114X(95)00100-D).
15. Legnani G, Casalo F, Righettini P, Zappa B. A homogeneous matrix approach to 3D kinematics and dynamics – II. Applications to chains of rigid bodies and serial manipulators. *Mechanism and Machine Theory* 1996; 31(5): 573-587, [https://doi.org/10.1016/0094-114X\(95\)00100-D](https://doi.org/10.1016/0094-114X(95)00100-D).
16. Mansfield N J. Human response to vibration. CRC Press LLC, Boca Raton, Florida, 2004, <https://doi.org/10.1201/b12481>.
17. Marques F, Flores P, Pimenta Claro J C, Lankarani H M. A survey and comparison of several friction force for dynamic analysis of multibody mechanical systems. *Nonlinear Dynamics* 2016; 86(3): 1407-1443, <https://doi.org/10.1007/s11071-016-2999-3>.
18. Morales D O, Westerberg S, La Hera P X, Mettin U, Freidovich L, Shiriaev A S. Increasing the level of automation in the forestry logging process with crane trajectory planning and control. *Journal of Field Robotics* 2014; 31(3): 343-363, <https://doi.org/10.1002/rob.21496>.
19. Papadopoulos E, Sarkar S. On the dynamic modeling of an articulated electrohydraulic forestry machine. in: *Proceedings of the 1996 AIAA Forum on Advanced Developments in Space Robotics*, WI, 1-2 August, 1996.
20. Papadopoulos E, Frenette R, Mu B, Gonthier Y. On the modeling and control of an experimental harvester machine manipulator. in: *Proceedings of IEEE/RSJ International Conference on Intelligent Robots and Systems*, Grenoble, France, 8-12 September, 1997, <https://doi.org/10.1109/IROS.1997.656611>.
21. Pennestri E, Rossi V, Salvini P, Valentini P P. Review and comparison of dry friction force models. *Nonlinear Dynamics* 2016; 83(4): 1785-1801, <https://doi.org/10.1007/s11071-015-2485-3>.
22. Posiadała B. Influence of crane support system on motion of the lifted load. *Mechanism and Machine Theory* 1997; 32(1): 9-20, [https://doi.org/10.1016/0094-114X\(96\)00044-4](https://doi.org/10.1016/0094-114X(96)00044-4).
23. Posiadała B. Modeling and analysis of the dynamics of load carrying system. in: *Proc. of World Congress on Engineering and Computer Science*, San Francisco, USA, 2012.
24. Posiadała B, Waryś P, Cekus D, Tomala M. The dynamics of the forest crane during the load carrying. *International Journal of Structural Stability and Dynamics* 2013; 13 (7), <https://doi.org/10.1142/S0219455413400130>.
25. Stribeck R. Die wesentlichen Eigenschaften der Gleit- und Rollenlager, *Zeitschrift des Vereines Deutscher Ingenieure* 2013; 46(36).
26. Urbaś A. Analysis of flexibility of the support and its influence on dynamics of the grab crane. *Latin American Journal of Solids and Structures* 2013; 10(1): 109-121, <https://doi.org/10.1590/S1679-78252013000100011>.
27. Urbaś A. Application of the Dahl friction model in the dynamics analysis of grab cranes, *MATEC Web of Conferences* 8347, 03008. doi: 10.1051/mateconf/2016 68303008, 2016.
28. Urbaś A. Computational implementation of the rigid finite element method in the statics and dynamics analysis of forest cranes. *Applied Mathematical Modelling* 2017; 46: 750-762, <https://doi.org/10.1016/j.apm.2016.08.006>.
29. Urbaś A, Harlecki A. Application of the rigid finite element method and the LuGre friction model in the dynamic analysis of the grab crane. in: *Proceedings of 4th Joint International Conference on Multibody System Dynamics*, Montreal, Canada, May 29-June 2, 2016.
30. Urbaś A, Szczotka M. Modelling friction phenomena in the dynamics analysis of forest cranes. *Engineering Transactions* 2016; 64(4): 393-400.
31. Szczotka M. Simulation and optimisation of the steering kickback performance. *Journal of Theoretical and Applied Mechanics* 2011; 49(1): 187-208.
32. Wittbrodt E, Szczotka M, Maczyński A, Wojciech S. Rigid Finite Element Method in Analysis of Dynamics of Offshore Structures. *Ocean Engineering & Oceanography*. Springer. Berlin-Heidelberg: 2013.

---

**Andrzej URBAŚ**

Department of Mechanical Engineering Fundamentals  
University of Bielsko-Biala  
Willowa 2, 43-309 Bielsko-Biala, Poland

**Marek SZCZOTKA**

Department of Transport  
University of Bielsko-Biala  
Willowa 2, 43-309 Bielsko-Biala, Poland

E-mail: [aurbas@ath.bielsko.pl](mailto:aurbas@ath.bielsko.pl), [mszczotka@ath.bielsko.pl](mailto:mszczotka@ath.bielsko.pl)

---